J MATER SCI 41 (2006) 3885–3897

Hydrothermal processing of barium strontium titanate sol-gel composite thin films

K. ZELONKA, M. SAYER*
Department of Physics, Queen's University, Kingston, Ontario K7L 3N6, Canada
E-mail: sayerm@physics.queensu.ca

A. P. FREUNDORFER
Department of Computer and Electrical Engineering, Queen's University, Kingston, Ontario K7L 3N6, Canada

J. HADERMANN
Department of Physics, Middelheim Campus, University of Antwerp, Groenenborgeriaan 171, Antwerp B-2020, Belgium

Published online: 12 April 2006

Stoichiometric barium strontium titanate (BST) films of composition $Ba_{0.7}Sr_{0.3}TiO_3$ with thickness >2 μm have been fabricated on Si/SiO_2/Pt substrates by hydrothermal sol-gel composite processing. This film deposition technique involves the treatment of a spun-on sol-gel composite film, formed from a suspension of a powder in an aqueous BST sol-gel, at temperatures from 100–200°C at a pressure of 1–15 atm. An initial hydrolysis procedure eliminates dissolution of the dried sol-gel during the hydrothermal treatment. Glancing angle X-ray diffraction shows excellent crystallinity and stoichiometry in the BST films with no evidence of new phases created during processing. Scanning electron micrography and atomic force microscopy show densification of the film structure and the development of a bridging microstructure. Transmission electron micrography indicates that while much of the sol-gel derived matrix phase is amorphous a more crystalline interface occurs with the powder particles. The relative permittivity and loss tangent of the films are measured using a parallel plate capacitor technique in the frequency range 1–100 kHz. At 100 kHz relative permittivities of the films range from $\varepsilon_r = 400$–1200 and loss tangents lie in the range $0.05 < \tan\delta < 0.10$, depending on the parameters of film preparation. The film structure and morphology and the electrical studies suggest that the microstructure of the films evolves by deposition of the sol-gel derived BST on the underlying powder, resulting in an electrically interconnected microstructure in which the sol-gel derived material bridges between the high permittivity powder particles.

1. Introduction

Barium strontium titanate (BST) is a material of interest for various applications due to its high relative permittivity and low loss tangent. There is a need to develop a method by which high-quality BST films may be deposited on temperature-limited substrates such as gallium arsenide (GaAs), polymers, and substrates with pre-patterned elements. In high frequency applications, GaAs is often preferable to silicon for use as a substrate due to its high electrical carrier mobility. These carriers react to high frequency microwaves and effectively switch electrical currents in communications systems faster than do silicon devices. GaAs can be exposed to temperatures <200°C for extended periods of time, but to a temperature of 350°C only for a time of less than 10 min. If exposed to temperatures over 350°C for longer periods, ohmic contacts and material stoichiometry begin to degrade. Conventional ceramic thin film fabrication techniques for BST, such as chemical vapour deposition, metallorganic decomposition, and sol-gel deposition with thermal sintering, generally require the sample and substrate to be subjected to temperatures of up to 750°C in order to crystallize the film

*Author to whom all correspondence should be addressed.
0022-2461
DOI: 10.1007/s10853-005-5525-4

and/or remove residual impurities. The substrates of interest in this paper cannot tolerate temperatures in this range. Many applications of BST as a high frequency (>20 GHz) dielectric layer also require films of thickness >1 μm. Most conventional film preparation methods cannot easily meet this objective. In this study we demonstrate that the hydrothermal processing of a sol-gel composite allows the deposition of high-quality BST films at temperatures below 200°C and with thicknesses >2 μm.

1.1. Hydrothermal processing of inorganic precursors

There have been attempts in the past to develop low-temperature deposition techniques for BST films. Various researchers have examined the possibility of converting metallic titanium layers and polycrystalline TiO_2 to crystalline BST by hydrothermal treatment of the film or powder in an alkaline aqueous solution containing Ba^{2+} and Sr^{2+} ions [1–7]. Several problems arise in the application of this method. Stoichiometric control of the final ceramic is difficult, as it depends on the incorporation of barium, strontium, and oxygen into the film from the surrounding solution by a diffusion controlled reaction. The relative and absolute amount of each element incorporated into the precursor is highly dependent on the processing conditions. The hydrothermally processed metallic films tend to remain highly enriched in Ti even after extended processing, causing them to remain highly conductive. High temperature processing is also still required to promote the adhesion of the precursor titanium layer. These issues result in hydrothermal treatment of Ti to form BST films being an unsatisfactory approach.

1.2. Hydrothermal crystallization of organic precursors

An alternate method for the low-temperature deposition of ceramic films has been outlined by Jianming Zeng *et al*. [8–10]. They have shown that it is possible to crystallize a titanate sol-gel thin film by subjecting it to hydrothermal conditions in an alkaline aqueous solution. It has also been demonstrated elsewhere that oxides may be precipitated from a sol-gel by treatment with an alkaline solution [11–13]. The presence of a highly alkaline solution leads to the removal of alkoxy ligands, forming $Ti(OH)_6^{2-}$. There is then a direct condensation between $Ti(OH)_6^{2-}$ and Me^{2+} ions, (where Me=Ba, Sr), to form the titanate compound. The formation of an inorganic compound (BST) by the processing of a sol-gel in film form by exposure to a high-pH environment may follow a similar reaction mechanism. The current study improves upon the technique of Zeng *et al*. by incorporating a BST powder into the sol-gel that is then hydrothermally treated. It has been found that this affords several significant advantages over the hydrothermal treatment of a simple sol-gel to which no powder has been added. The hydrothermal treatment of a sol-gel composite rather than a simple sol-gel allows for better stoichiometric control of the final film, promotes better adhesion of the film to the substrate, leads to a smooth transition between the powder and sol-gel derived material, and allows for the possibility of depositing a thicker film than with a simple sol-gel with no powder.

1.3. Crystallization chemistry in the sol-gel composite hydrothermal process

Work by Bucko *et al*. [14] on the hydrothermal crystallization of zirconia powder suggests a possible mechanism by which crystallization of a sol-gel composite in an alkaline aqueous solution may be enhanced in comparison with that of a simple sol-gel. In the case of zirconia, two possible mechanisms for crystallization were initially suggested. Nishizawa *et al*. [15] postulated that there occurred a spontaneous coalescence of highly ordered zirconia crystallites into elongated monoclinic crystals, with no dissolution/recrystallization occurring. Alternately, Tani *et al*. [16] suggested that a dissolution/precipitation process was entirely responsible. Búcko *et al*. showed that both of these processes act. A zirconia gel, zirconia crystallites, and a zirconia gel containing zirconia crystallites were separately treated hydrothermally in NaOH. The kinetics of the reaction in the third (mixed) case were the fastest. Both growth of new crystallites, and dissolution/recrystallization of existing crystals were observed. The titanate powders used in BST sol-gel composite processing behave similarly to the crystallites used to seed the zirconia gel, in that they act as dissolution/recrystallization sites.

1.4. Details of the current study

In the present study, BST sol-gel composite films are processed by a hydrothermal treatment to develop and evaluate a technique for the deposition of high-quality BST films at temperatures below 200°C. This paper discusses the experimental methods used to fabricate the sol-gel composite films, including the preparation and deposition of the sol-gel composite and the details of its hydrothermal treatment. The crystallinity and stoichiometry of the film as a whole are examined using X-ray diffraction (XRD) and those of the matrix phase are examined using transmission electron microscopy (TEM). The microstructure of the films is investigated using scanning electron microscopy (SEM), and atomic force microscopy (AFM). The low-frequency electrical response of the films, including relative permittivity and loss tangent, are determined using a parallel plate capacitor technique. Illustrative examples are included here. A detailed study of the low-frequency behaviour of the films and of the high frequency (20–40 GHz) response of the films will be presented elsewhere.

2. Experimental method

2.1. Sol-gel composite preparation

An acetic acid-based sol-gel with a barium to strontium ratio of 70:30 was used. The precursor sol-gel

TABLE I Reagent masses used to fabricate BST sol-gel

Reagent	Mass used (g)
Titanium (IV) Butoxide	3.66
Acetic acid	8.00
Methanol	3.00
Deionized water	6.00
Barium acetate	1.92
Strontium acetate (0.5 H_2O)	0.69

was produced by dissolving appropriate amounts of barium acetate ($(CH_3COO)_2Ba$, BDH) and strontium acetate ($(CH_3COO)_2Sr{\cdot}0.5H_2O$, Alfa Aesar) in deionized water. This solution was added to a mixture of titanium butoxide ($Ti[O(CH_2)_3CH_3]_4$, Aldrich Chemical), acetic acid (Aldrich Chemical), and methanol (Fisher Chemical), and agitated, producing a clear, colourless liquid. The sol-gel was stable for three days. This stability time could be increased to seven days by a three-fold increase in the amount of methanol added. Table 1 shows the mass of each reagent used. The flowchart in Fig. 1 shows the order of mixing.

A BST powder of the same composition was prepared by combining appropriate amounts of barium carbonate (Aldrich Chemical), strontium carbonate (Fisher Chemical), and titanium dioxide powder (Fisher Chemical). The powders were ball-milled dry with alumina balls to promote mixing, fired for 20 h at 1100°C in an alumina crucible, and then ball milled again to break up the resulting mass of BST. This produced a powder with particles with an average diameter of 0.3 μm, as determined from SEM images.

Adding the BST powder to the sol-gel produced the sol-gel composite solution. In this study, unless otherwise stated, the ratio of the mass of the powder to the mass of the sol-gel is 1:1. The mixture was agitated in an ultrasonic mixer for five hours in order to break up any agglomerated particles and to distribute the powder throughout the sol-gel.

2.2. Film deposition

Films were fabricated by spin-coating the sol-gel composite solution onto platinized Si/SiO_2. Each layer deposited was dried on a hot plate at 150°C for 10 min, and hydrolyzed above a hot water bath for 10 min to prevent dissolution upon immersion in the hydrothermal solution. For the sol-gel composite solution with a mass ratio of powder to sol-gel of 1:1 used, a spin-rate of 3000 rpm for one minute produced a single layer 2.6 μm thick. Variations in the constituents of the sol-gel composite solutions (such as varying the relative amount of powder) required the spin-rate used for deposition to be altered to maintain a constant film thickness between samples.

2.3. Hydrothermal processing

The hydrothermal solution was prepared by dissolving the appropriate amounts of $Ba(OH)_2{\cdot}8H_2O$ and $Sr(OH)_2{\cdot}8H_2O$ (Aldrich Chemical Company, Inc.) in deionized water which had been boiled for 10 min to remove dissolved CO_2. The dissolution was carried out under a nitrogen atmosphere to prevent the precipitation of Ba^{2+} and Sr^{2+} from the solution as carbonates. Once

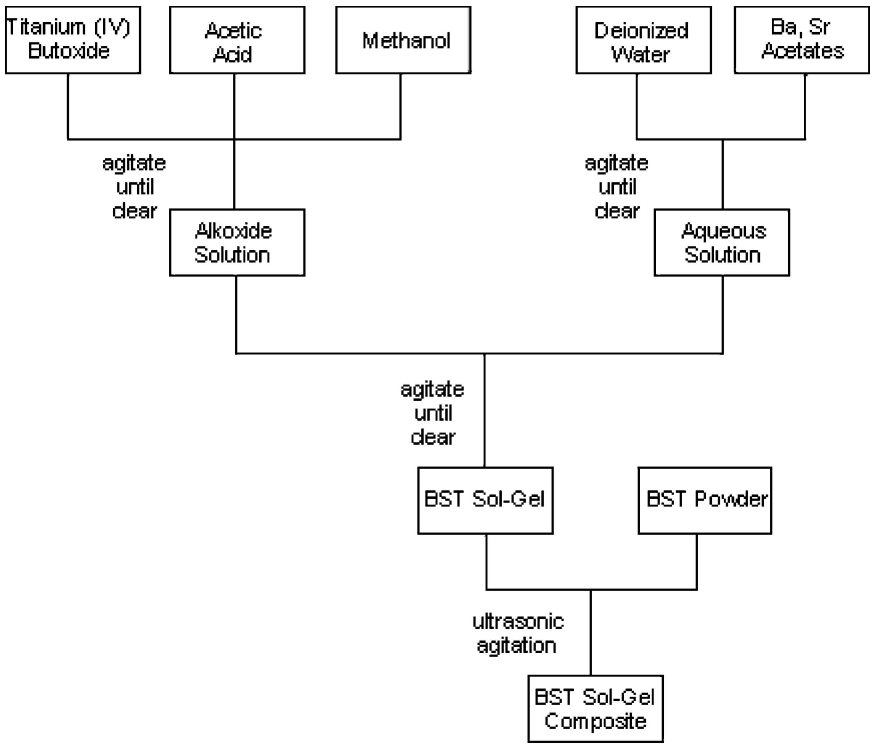

Figure 1 Flowchart of BST sol-gel composite production.

dissolution of the hydroxides was complete, the sample was transferred into the hydrothermal solution, which was contained in a Teflon vessel, and was sealed inside an autoclave. The vessel was purged with nitrogen, again to prevent the precipitation of the anions as carbonates. The pressure inside the vessel was autogeneous, and close to the vapour pressure of pure water. The temperature of the vessel was controlled via a feedback loop to an external heater. Typical processing temperatures were between 100°C and 200°C, yielding pressures between 1 and 15 atmospheres. After the allotted processing time and cooling for 1 h, the vessel was opened; the sample was removed from the solution, rinsed in deionized water, and dried in a stream of air.

2.4. Analysis techniques

X-ray diffraction (XRD) studies were carried out to examine the crystallinity and composition of the starting powders and final films. Powder studies were completed on a Phillips X'Pert XRD Analyzer with Cu Kα radiation at a wavelength of 1.54 Å and film studies were performed using a Rigaku XRD analyzer with Cu Kα radiation or Cr Kα radiation with a wavelength of 2.29 Å. In the case of films, a glancing angle of incidence (2°) of the beam was used.

Film thickness measurements were made by a force feedback tip, the Rank Taylor Hobson 'Talystep' profilometer. The tip of the device is dragged over the surface of the film, and the force on the tip is monitored. This is calibrated to give a measurement of the thickness of the film under test.

Scanning electron microscopy (SEM) using a JEOL 740 SEM and atomic force microscopy (AFM) using a NanoScope Multimode AFM were used to examine the microstructure of the films. Transmission electron microscopy was employed to examine the crystallography of the matrix phase and its interface with the powder particles. Samples for examination were prepared by grinding the substrate down to a thickness of 20 microns, placing a carbon grid and protective glass coating on the film side, and then ion milling the substrate in a dual gun ion mill with the beams striking the surface at an angle of 10 degrees until electron transparency could be achieved. Given the particulate nature of the films this meant that the upper particle layers were displaced from the matrix leaving remnants of the film structure to be observed. This was sufficient to provide information on the crystallinity of the matrix material and of the nature of its interface with the powder particles.

The relative permittivity and loss tangent of the BST films were determined by a parallel plate capacitor technique. A platinum layer on the substrate served as a bottom electrode, and a gold top electrode was deposited on the processed BST film under test by vacuum evaporation through a shadow mask. The top electrodes were circular, with a radius of 0.25 mm. Capacitance and loss tangent measurements were made between 1 and 100 kHz using a Hewlett-Packard 4284A Precision LCR Meter.

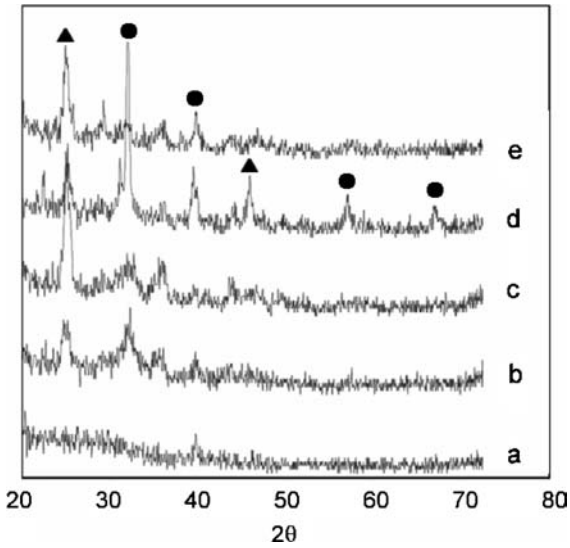

Figure 2 The effect of hydrothermal processing on the composition of non-composite sol-gel BST films. Each film is processed at 150°C for 2 h. The concentration of the hydrothermal solution is varied, (a) 0M (b) 0.1 M (c) 0.2 M (d) 0.3 M (e) 0.5 M. Circles indicate BST peaks. Triangles indicate $(Ba,Sr)CO_3$ peaks.

3. Results

3.1. BST sol-gel to which powder has not been added

XRD spectra of sol-gel BST films to which no powder had been added (non-composite) which were hydrothermally processed in solutions of various concentrations are shown in Fig. 2. All films were processed at 150°C for 2 h. At concentrations of 0.1–0.3 M, the BST(111) peak is evident. The film processed at 0.3 M also shows additional BST peaks, indicating a greater degree of crystallization over films processed in lower concentration solutions. Only one BST peak is evident in the spectrum of the film processed at 0.5 M, as the film experienced significant desorption, likely due to the rapid attack of hydroxide ions on the gel, not allowing sufficient time for re-deposition of the crystalline species before transport from the substrate/solution interface occurred.

In all films except for the one treated in pure water, carbonate peaks (JCPDS 5-418, 5-378) that are large in comparison to the BST peaks (JCPDS 13-522, 34-411, 39-1395) are evident. This indicates that the crystalline carbonates arise primarily through precipitation of carbonates from the solution rather than from the residual carbon in the sol-gel.

3.2. Benefits of using a sol-gel composite over a simple sol-gel

Fig. 3 shows a comparison between the effects of hydrothermal processing on the composition of composite and non-composite BST films. While the composite films show no shift in peaks away from that of the powder alone, the non-composite films show a definite peak shift. The sample treated in a $Ba(OH)_2{\cdot}8H_2O$ solution shows peaks

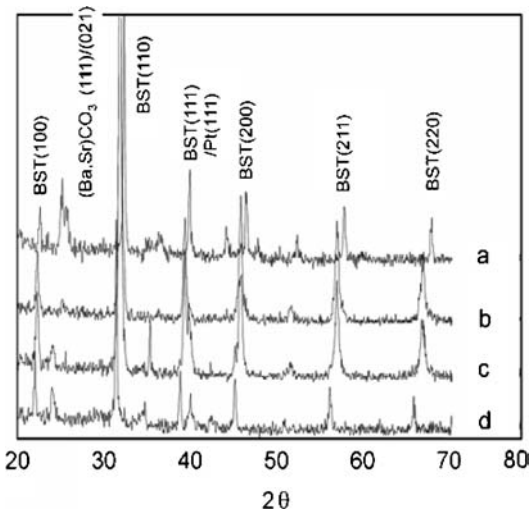

Figure 3 The effect of hydrothermal processing on the composition of composite and non-composite sol-gel BST films. All films processed in 0.3 M solution at 150°C for 2 h, (a) sol-gel in $Sr(OH)_2{\cdot}8H_2O$ solution, (b) sol-gel composite in $Sr(OH)_2{\cdot}8H_2O$ solution, (c) sol-gel composite in $Ba(OH)_2{\cdot}8H_2O$ solution, (d) sol-gel in $Ba(OH)_2{\cdot}8H_2O$ solution.

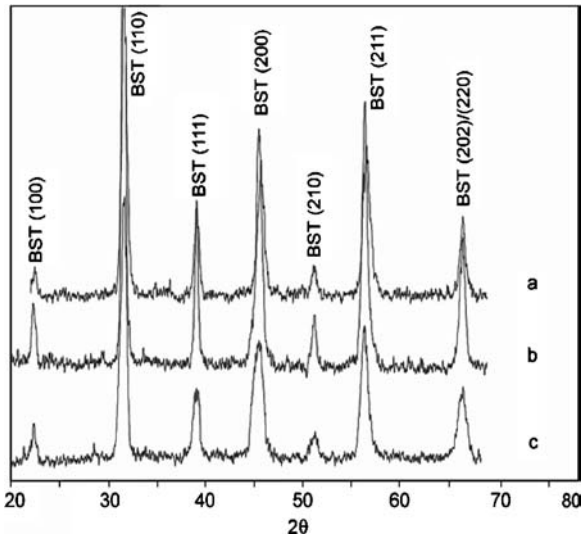

Figure 4 The effect of hydrothermal processing on the composition of BST powders. All films processed in 1.0 M solution at 200°C. Duration time: (a) 5 h (b) 24 h (c) 48 h.

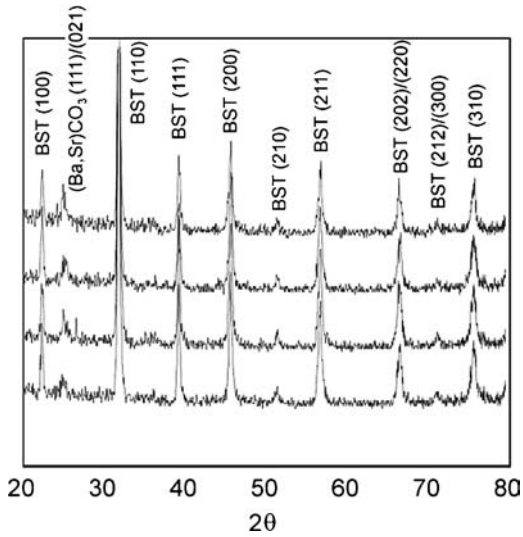

Figure 5 The maintenance of composition of sol-gel composite films in various concentration solutions (top to bottom: 0.1, 0.3, 0.5, and 1.0 M), processed for 48 h at 200°C.

shifted to lower 2θ values, while the sample treated in a $Sr(OH)_2{\cdot}8H_2O$ solution has peaks shifted to higher angles. This is consistent with the film becoming more Ba or Sr rich in composition during the hydrothermal treatment, depending on the contents of the solution. It is expected that the shift in peaks of the non-composite samples is a result of a compositional change rather than residual stresses induced in the lattice during crystallization. Were the shift due to stress in the lattice, the shift in peaks would be expected to be all in the same direction, which they are not. In the case of the composite, the powder does not change in composition, even at extended reaction times in a high-concentration solution (1.0 M $Ba(OH)_2{\cdot}8H_2O$ or $Sr(OH)_2{\cdot}8H_2O$), at a high temperature (200°C), as shown in Fig. 4. Thus, the overall composition of the sol-gel composite films remains constant, as shown in Fig. 5, unlike the composition of simple sol-gel films.

Control of the stoichiometry of BST is important for control of its electrical behaviour. The Curie temperature of BST is strongly dependent on the ratio of Ba to Sr, as $BaTiO_3$ and $SrTiO_3$ have widely differing Curie temperatures of 395 K and ~20 K respectively. The Curie temperature of the BST film in turn determines its room temperature permittivity. The ratio of Ba to Sr also affects the loss tangent of the film although at high frequencies structural factors and internal barriers probably have the most significant effect.

3.3. Microstructure

The microstructure of the raw sol-gel composite film is examined by SEM in Fig. 6. The powder phase is clearly surrounded by the dried sol-gel matrix. Figs.7–9 show microstructural changes of the film as a function of process time, solution concentration, and process temperature. As processing continues, the matrix phase becomes less evident indicating that it has been removed, converted to crystalline BST, or has become closely integrated with the powder. The SEM images indicate that as the conditions are enhanced to facilitate crystallization, the density of the overall layer increases. If the sol-gel component were just removed or dissolved by the hydrothermal process, the powder would not adhere to form a coherent film and the observed increase in density would not take place. The observation that crystalline BST is present in hydrothermally treated non-composite BST films suggests that the sol-gel phase is converted into crystalline BST by the hydrothermal process. Nucleation and growth of BST from the sol-gel is likely to be most favoured on the surface of BST powder particles acting as seeds, rather

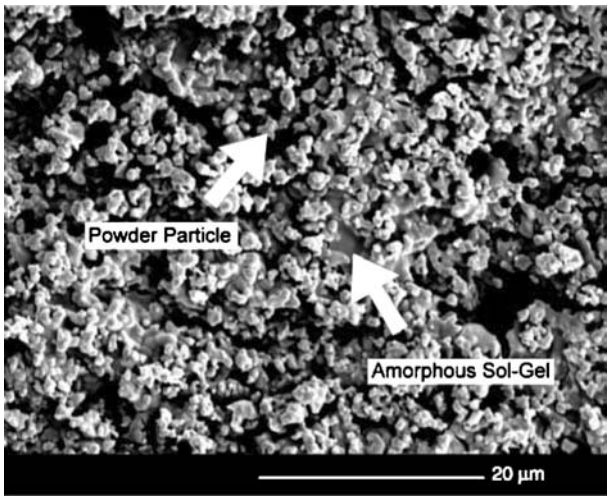

Figure 6 The BST sol-gel composite fihn as deposited, before hydrothermal treatment. Both the powder phase and the surrounding sol-gel matrix are evident.

than in the body of the interparticle sol-gel matrix. When the concentration of the hydrothermal solution and the processing temperature are kept constant, an increase in process time promotes the growth of finer structures in the film (Fig. 7). This suggests that in addition to the direct conversion of the sol-gel to crystallized BST, a dissolution-recrystallization process occurs. At 1 h there is no amorphous phase evident between the crystalline elements, but at later times this space is filled. This is hypothesized to be BST that has been dissolved and re-crystallized to form the new microstructure. A more concentrated hydrothermal solution promotes the growth of denser, finer structures in the film (Fig. 8). The condensation of the sol-gel to crystalline BST is promoted in high pH solution due to increased attack on the sol-gel by OH^- ions. A higher process temperature tends to result in more extensive growth of the film (Fig. 9), suggesting that the reaction kinetics are faster at higher temperatures.

The morphology of the structures resulting from this process were initially examined by an evaluation of the surface morphology using atomic force microscopy. In a film prior to processing, Fig. 10 shows powder particles almost completely surrounded by dried matrix film as in the SEM image of the raw film (Fig. 6). The mass ratio of powder to sol-gel is 1:2. Fig. 11 shows AFM images of the progressive growth of bridging structures in films with various powder loadings and process times. All films except for (b) are processed for 3 h in 0.3 M $(Ba,Sr)(OH)_2 \cdot 8H_2O$ solution at 150°C. The sample in (b) is processed for only 1 h. The powder to sol-gel ratios of the samples in Fig. 11 are: (a) l:10 (b) l:2 (c) 1:2 (d) 1:1. A more defined morphology results following processing as the sol gel matrix shrinks around the powder to form bridges between particles. In the cases of higher powder

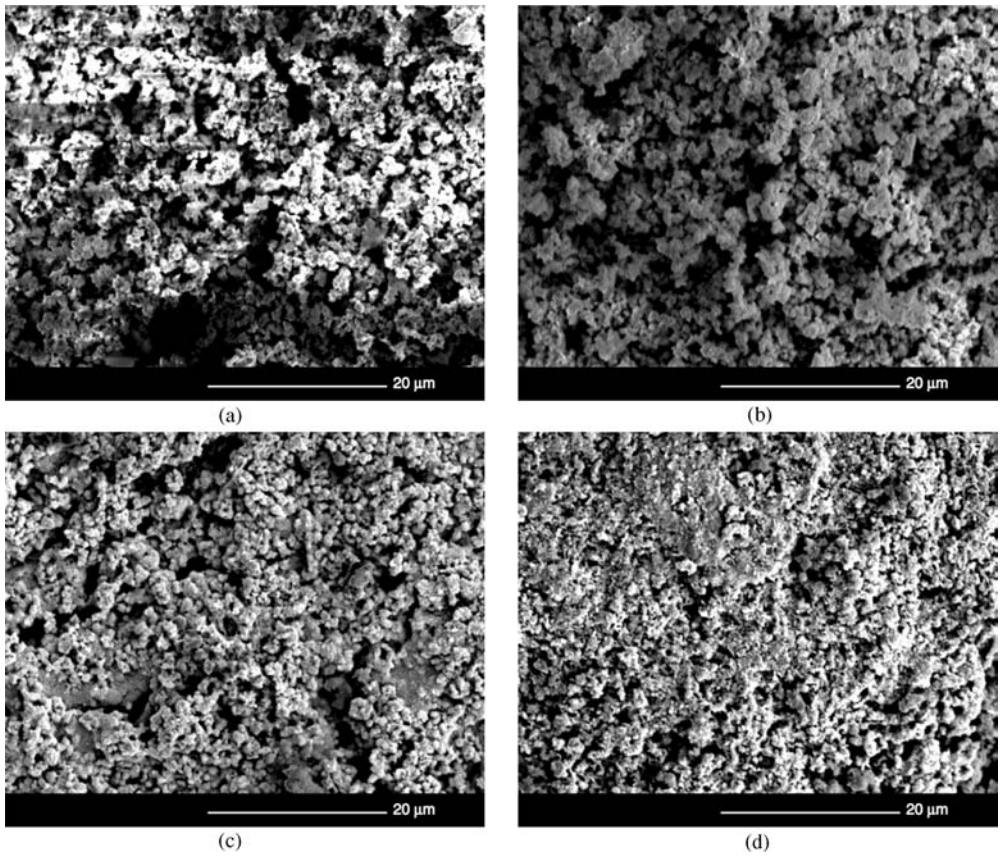

Figure 7 The variation of BST film microstructure with process time. All samples are processed in 0.1 M $(Ba,Sr)(OH)_2 \cdot 8H_2O$ at 150°C. (a) 1h (b) 2 h (c) 5 h (d) 20 h.

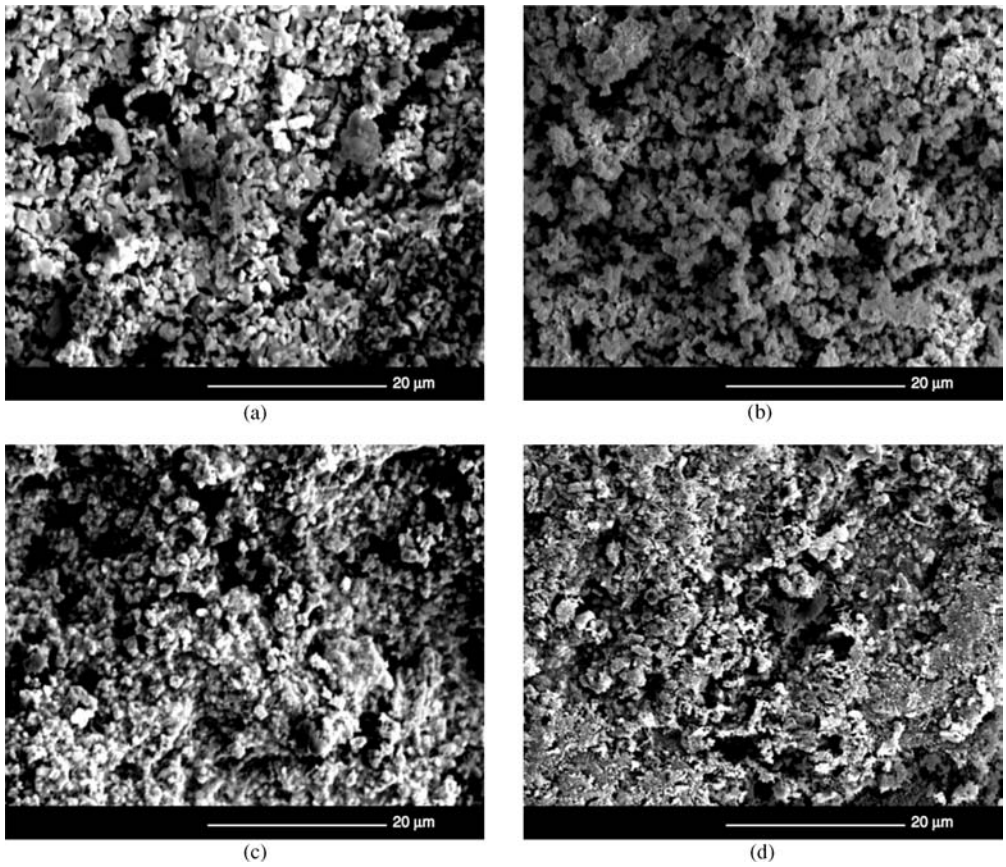

Figure 8 The variation of BST film microstructure with hydrothermal solution concentration. All samples are processed for 2 h at 150°C. (a) 0M (b) 0.1M (c) 0.5 M (d) 1M.

loadings and longer process times, the connectivity of the powder phase becomes greater.

The development and crystallography of such bridges is seen clearly in the TEM images of sections of the films shown in Fig. 12. Fig. 12a is a low magnification view of a segment of the film containing particles with linking matrix phase. Fig. 12b is a high-resolution image of a section of the interface crossing from the powder material into the matrix. The existence of a local crystallographic structure is shown by lattice imaging lines, while amorphous material is seen as a random set of disconnected whorls. Much of the matrix material far from the interface with the powder appears to be amorphous. However, in Fig. 12b lattice structures extending into the material from the adjacent powder structure indicates some degree of epitaxy. There is also evidence of crystallization far away from the interface as indicated by areas of the matrix containing lattice lines. Areas of 12b outlined in black are crystalline and show lattice lines at higher magnification. The corner denoted *A* is the same in 12a and 12b for orientation. 12(b.1), (b.2), and (b.3) show enlarged sections of 12 (b) as denoted by numbers 1, 2, and 3. The contrast in these areas in 12b has been enhanced to indicate the region enlarged. In 12(b.l) lattice lines are evident in a section of the sol-gel derived material far away from the interface with the powder. 12(b.2) shows a crystalline portion of the sol-gel derived matrix in close proximity to a powder particle. In this case there is a large degree of lattice mismatch between the powder and the sol-gel derived material. In contrast Fig. 12(b.3) shows lattice lines extending from the powder particle into the sol-gel derived material. This indicates that growth of the sol-gel derived crystalline BST is at least in part epitaxial on the surface of the powder particles. Fig. 12(b.4) shows an amorphous region of the film. A related observation from Fig. 12a is that the transition between the matrix and the powder is smooth with no evidence of physical discontinuities. Such a transformation may be expected if it is the result of a dissolution-precipitation sequence even if subsequent crystallization did not take place.

3.4. Low-frequency electrical characterization

The frequency dependence of the relative permittivity (ε_r) and loss tangent ($\tan\delta$) of sol-gel composite hydrothermal BST films were examined in the frequency range 1 to 100 kHz by forming a parallel plate capacitor with the BST films as the dielectric. Here we present an example of typical permittivity measurements so that they may be considered in conjunction with the variation in film microstructure. A detailed study of the low-frequency electrical response of the films will be presented elsewhere.

Fig. 13 shows the variation of relative permittivity with process duration. All films are processed at 150°C in 0.5 M $(Ba,Sr)(OH)_2 \cdot 8H_2O$ solution. As the process time

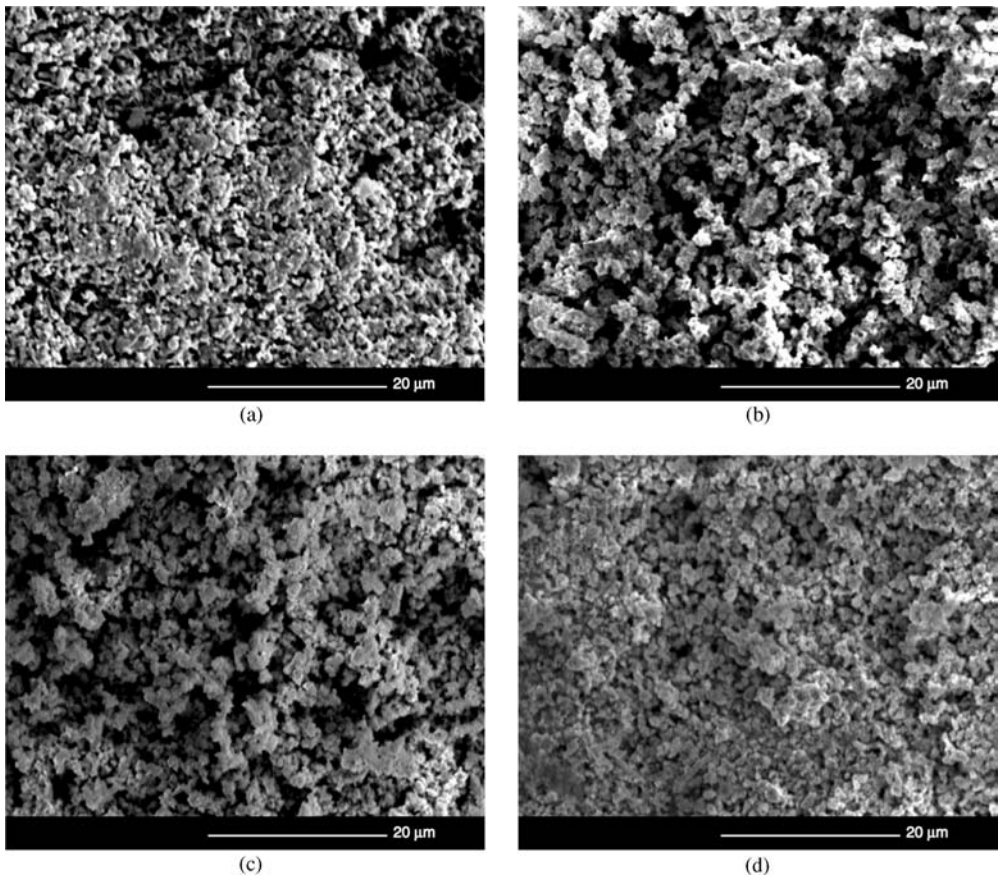

Figure 9 The variation of BST film microstructure with process temperature. All samples are processed in 0.1 M $(Ba,Sr)(OH)_2 \cdot 8H_2O$ for 2 h. (a) 50°C (b) 100°C (c) 150°C (d) 200°C.

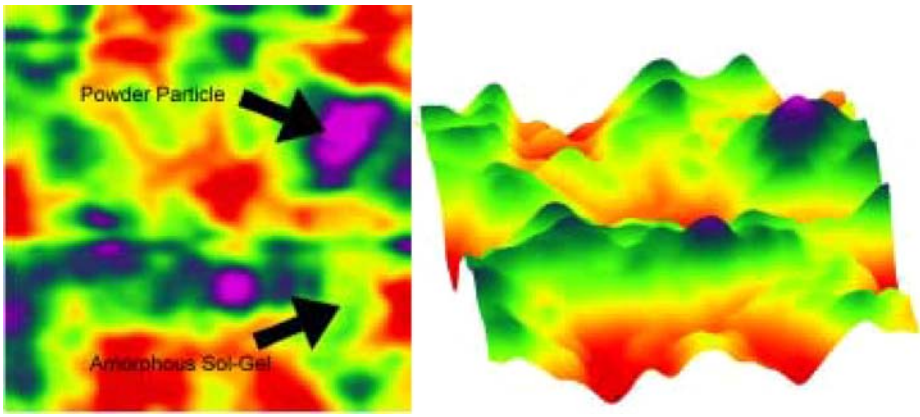

Figure 10 AFM image of raw films. Powder loading 1:2. 2 μm square, height variation 100 nm.

is varied between 1 h and 20 h, the relative permittivity increases from about 300 to about 1000. Such an increase in permittivity would be expected based on the variation of film microstructure with increased process time (Fig. 7). At 100 kHz, loss tangents of the films are in the range $0.05 < \tan\delta < 0.10$.

4. Discussion

4.1. Advantages of hydrothermal sol-gel composite processing

The technique of hydrothermal sol-gel composite processing outlined here has several significant advantages over other film deposition techniques. It does not involve temperatures in excess of 200°C like many other deposition techniques (such as CVD, metallorganic decomposition, and conventional sol-gel processing). This makes it compatible with many temperature-limited substrates, such as GaAs and polymers. The technique also allows for better stoichiometric control, better adhesion, and (as will be outlined elsewhere) better electrical characteristics over frequencies up to 40 GHz than films fabricated by other low-temperature techniques (such as hydrothermal processing of Ti or simple sol-gels).

4.2. Limitations on hydrothermal processing parameters

The hydrothermal conditions under which the film is crystallized have a significant impact on the microstructure of the final film. In particular, crystallization and densification of the films is promoted by a hydrothermal process with higher temperature, higher concentration of the hydrothermal solution, and a longer process time. An increase in the permittivity of the film is also seen under these conditions. There are, however, limits placed on the hydrothermal processing parameters as a result of other concerns. Firstly, the temperature at which the film is processed cannot exceed 200°C in order to ensure compatibility of the process with temperature-limited substrates such as GaAs. Secondly, if the concentration of the hydrothermal solution exceeds 0.5 M, then the adhesion of the BST film to the substrate is compromised, making the repeatable deposition of large-area films difficult. Lastly, extended process times tend to compromise the adhesion of the BST film, and may have detrimental effects on the substrate material or other pre-patterned components subjected to the hydrothermal process. Film adhesion tends to become an issue for films processed for longer than 3 h. This may be due to continued dissolution and recrystallization of the film that may weaken the bond between the film and the substrate.

The mass ratio of powder to sol-gel in the sol-gel composite also affects the microstructure of the final film. The higher the relative amount of powder, the denser and more highly interconnected the final film material, and the higher the relative permittivity. If, however, the mass ratio of powder to sol-gel exceeds 1:1, it becomes increasingly difficult to distribute the powder evenly in the sol-gel, and the film obtained by the spin-on process is not of uniform thickness.

The TEM observation that much of the bridging material away from the interface with the powder is amorphous has to be taken into account. The width of the XRD lines for the hydrothermally treated non-composite sol-gel films shown in Fig. 2 indicates that the crystallization process leads to a less well defined structure than produced by conventional sintering at higher temperatures. This is consistent with the average structure noted by TEM. An amorphous phase may have smaller permittivity than expected from crystalline material. However, the purpose of the bridges is primarily to form an electrical interconnection across the multiple small interfaces between powder grains which are in close proximity. Considerations of

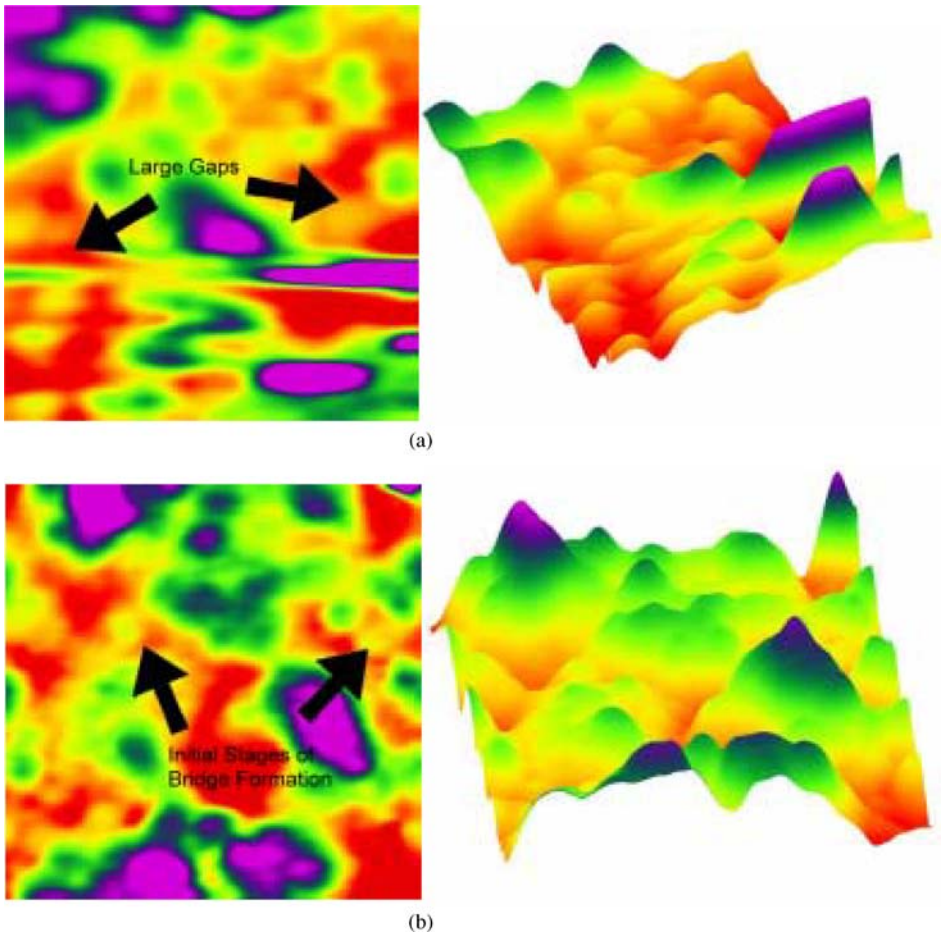

Figure 11 AFM images showing variation of microstructure with powder loading and process time. All films except (b) processed for 3 h in 0.3 M $(Ba,Sr)(OH)_2 \cdot 8H_2O$ at 150°C. (b) processed for 1 h 2 μm square, height variation 100 nm. Powder loadings: (a) 1:10, (b) 1:2, (c) 1:2 (d) 1:1.

(*Continued on next page.*)

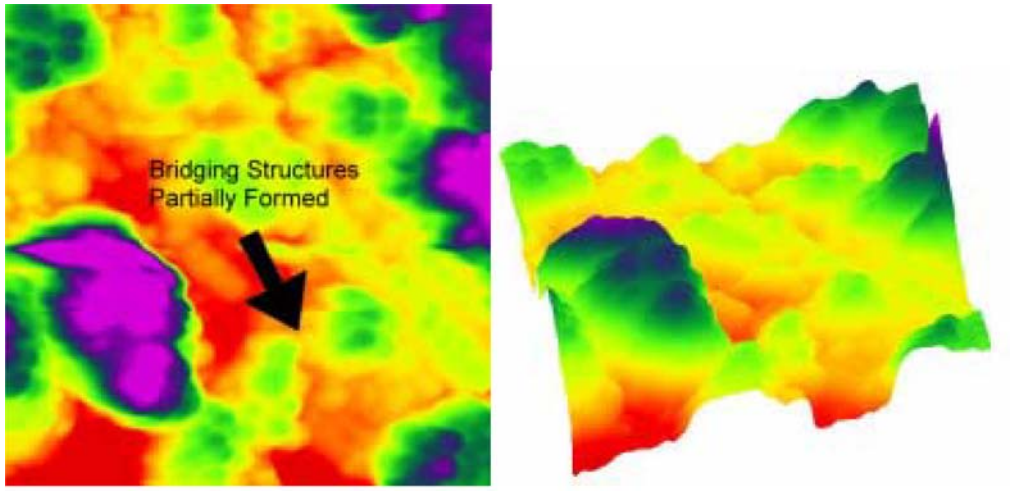

(c)

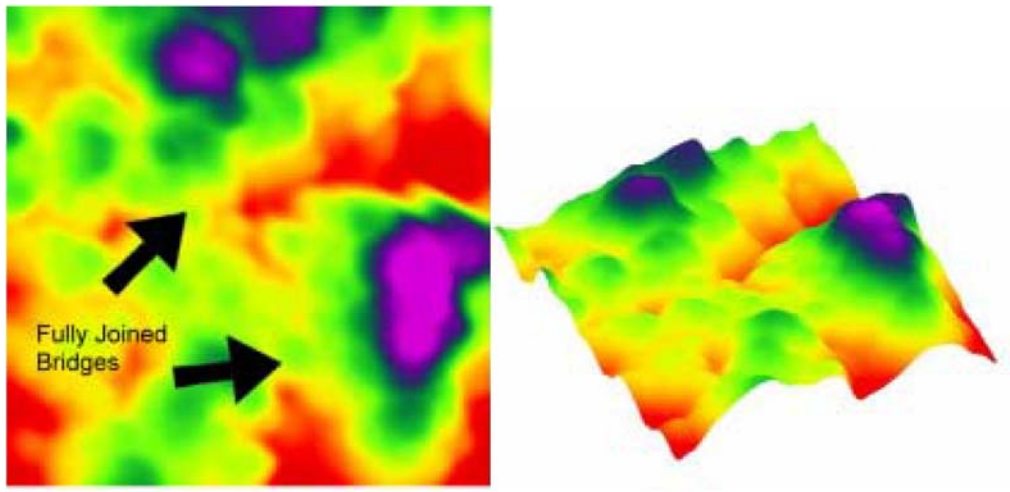

(d)

Figure 11 Continued.

spatial resolution make it difficult to probe this interfacial region. However, the more important function may to be to eliminate material discontinuities at the interface which lead to large electrical barriers and high dielectric losses. In these terms, the smooth material transition from powder to matrix phase observed in TEM of the interface suggests that the dissolution-precipitation process hypothesized to take place during hydrothermal processing plays an effective role in facilitating this function.

4.3. Film thickness

The thickness of the deposited film may be controlled in several ways. The viscosity of the sol-gel composite is determined by the constituents of the sol-gel and by the amount of powder added. These in turn affect the thickness of the final film. The spin rate used to deposit the sol-gel composite may also be used to determine the thickness of the film. Multiple layers of sol-gel composite may be deposited to build up a thicker film, as long as they are hydrolyzed between depositions to prevent dissolution. The thicker the layer deposited in one coat, the more likely the film is to crack during drying.

The limitation on the maximum thickness of the film is primarily imposed by the effect of the hydrothermal process on the film. Films with thickness in excess of $\sim$5 μm tend to lift off the substrate during the hydrothermal process. The limitation on the minimum thickness of the film is determined by the size of the powder used in the sol-gel composite. In this study, the BST powder had an average diameter of 0.3 μm, which led to films with thickness of less than 1 μm not having uniform thickness.

In conventional thermal processing of a sol-gel composite a decrease in film thickness occurs upon firing. If, however, the sol-gel composite is crystallized by a hydrothermal process, the thickness after processing is the same as the thickness of the dried but uncrystallized film. This is a convenient feature, as deposition parameters may be optimized for a desired film thickness without having to hydrothermally crystallize each film. It is hypothesized that this lack of shrinkage is due to the in situ conversion of the amorphous sol-gel to a crystalline form by a chemical process.

4.4. Initial film hydrolysis

An important aspect of successful film deposition by the hydrothermal sol-gel composite method is the partial hydrolysis of the film in water vapour prior to hydrothermal processing. If this is not done, then the sol-gel composite film will be removed by the next layer deposited, or by the hydrothermal solution. The effect of water vapour on the raw film has not been studied here, but the effect of water vapour on other films indicates that it does have an effect on the crystallization behaviour of sol-gel films in many cases. For instance, work by Imai *et al*. [15] on the preparation of anatase coatings from titanium dioxide

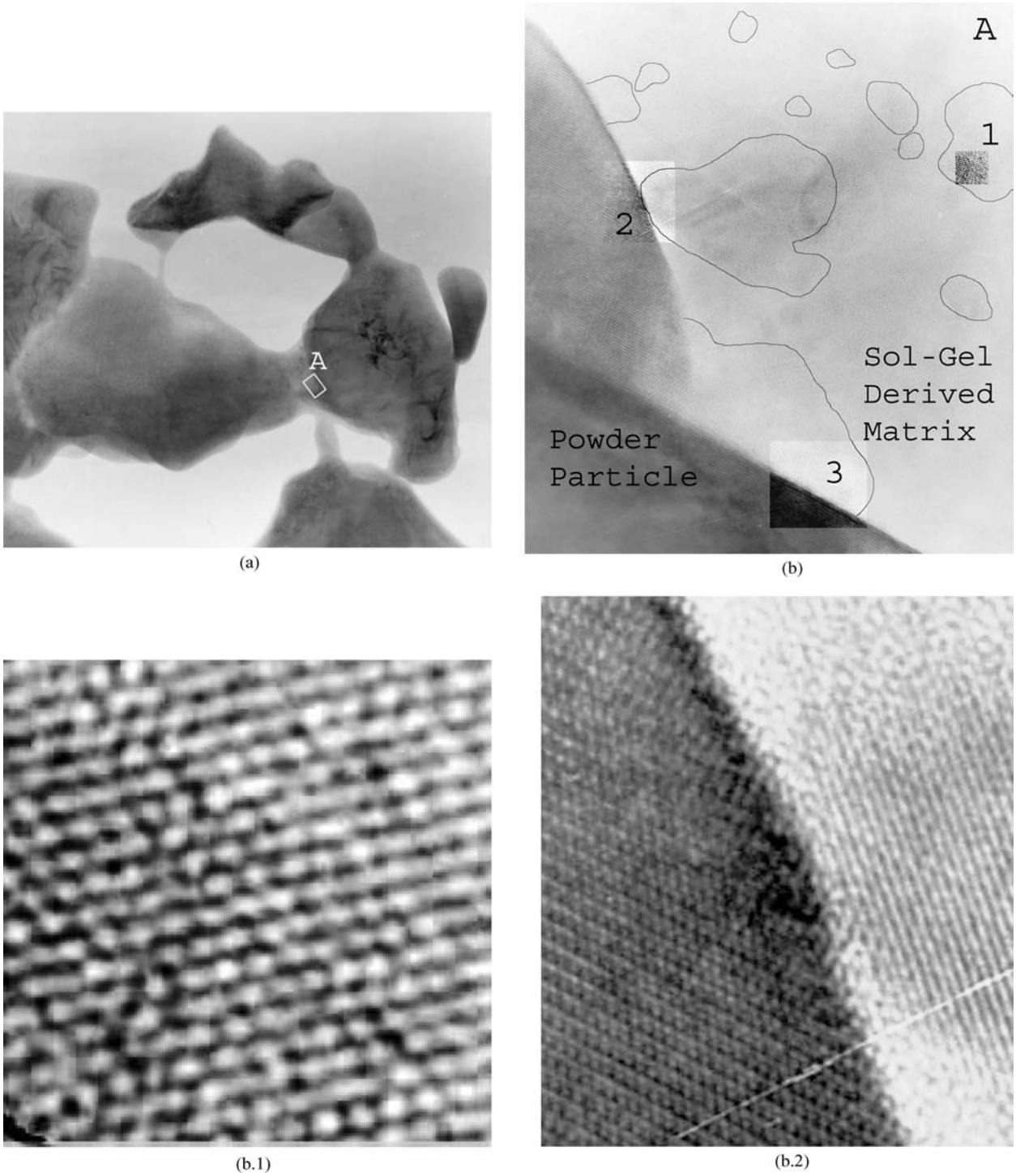

Figure 12 TEM images of a hydrothermally processed BST film. (a) shows a wide view in which several particles joined by sol-gel derived material are evident. (b) shows an enlarged portion of (a) as indicated by the white rectangle. The corner denoted *A* is the same in each image. (b.l), (b.2), and (b.3) show enlarged sections of (b) as denoted by numbers 1, 2, and 3. The contrast in these areas in (b) has been enhanced. Areas in Fig. 12(b) outlined in black show evidence of lattice lines at higher magnification. Fig. 12(b.4) shows an amorphous region of the film.

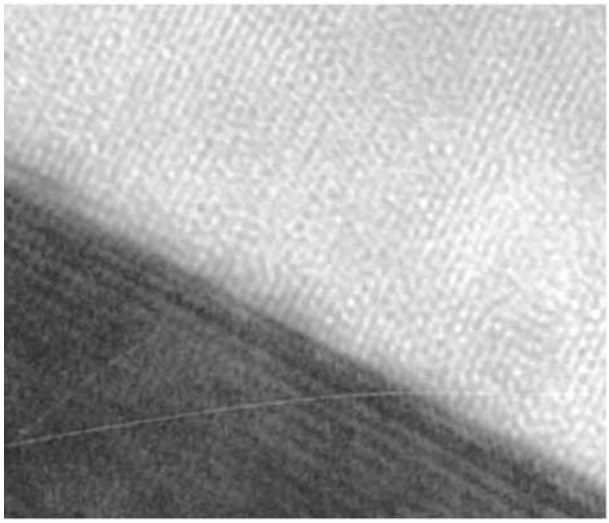

(b.3)

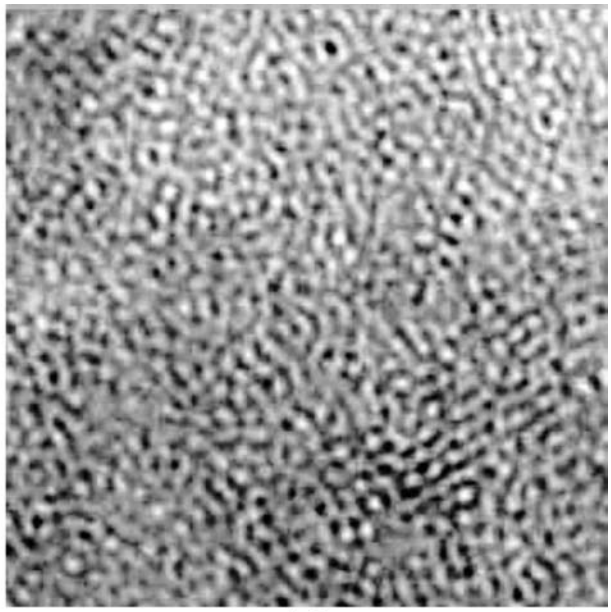

(b.4)

Figure 12 Continued.

and titanium dioxide-silica sol-gels indicates that exposure of a gel to a high humidity environment affects the crystallization behaviour of the ceramic. Similarly, Matsuda *et al*. [16, 17] reported structural changes in sol-gel-derived SiO_2 and SiO_2 containing TiO_2 in a high humidity environment at temperatures below 100°C. The crystallization process in humid atmospheres is hypothesized to be a hydrolysis reaction due to the water vapour, which causes a rearrangement of the gel network with cleavage of Ti–O–Ti bonds, followed by a condensation reaction which gives rise to the crystalline film. Crystallization of TiO_2 in a solvent or of gel films is thought to occur through dissolution in adsorbed water, migration, and subsequent recrystallization [14]. It has also been shown that curing in a humid atmosphere promotes the removal of alkoxy groups over curing in a dry environment, at temperatures as low as room temperature [18]. Structural changes similar to those outlined here are suspected to occur in the raw BST sol-gel composite films upon exposure to a high-humidity environment.

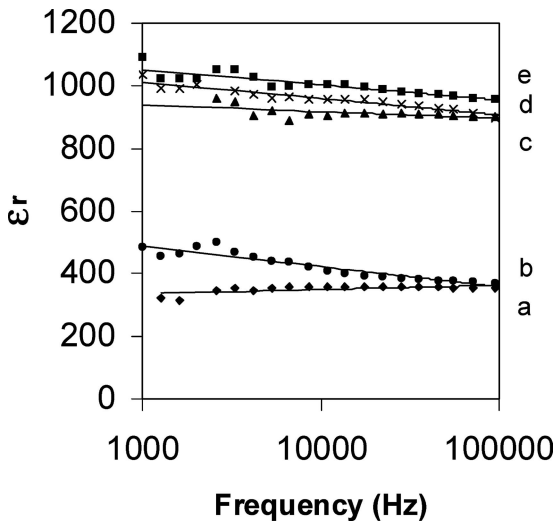

Figure 13 Variation of the dielectric constant of BST films with process time. All films processed in 0.5 M $(Ba,Sr)(OH)_2 \cdot 8H_2O$ for at 150°C. a) unprocessed film b) 1 h c) 2 h d) 5 h e) 20 h.

4.5. Possible applications of the sol-gel composite hydrothermal method

The use of the sol-gel composite hydrothermal method is not necessarily limited to BST films. In principle, any sol-gel that may be crystallized by a hydrothermal process may be mixed with any powder that can withstand hydrothermal processing for use as a sol-gel composite. As it is the sol-gel and powder in combination that determine the behaviour of the final film, this may allow the sol-gel composite hydrothermal process to be a useful technique for many applications.

5. Conclusions

A barium strontium titanate sol-gel composite may be processed to have high permittivity and relatively low dielectric loss at high frequency by subjecting it to hydrothermal processing in an alkaline aqueous solution. The final stoichiometry of the film is determined primarily by the powder constituents of the film, resulting in a better ability to control the stoichiometry of the film than in the case of a simple sol-gel film without powder. The effects of varying process time, temperature, and concentration of hydrothermal solution have been examined. Relative permittivities of $\varepsilon_r = 400$–1200 have

been measured in the frequency range 1–100 kHz. Loss tangents at 100 kHz lie in the range $0.05 < \tan \delta < 0.10$. The combination of morphology and crystallization studies in association with electrical measurements suggests that the hydrothermal process leads to effective electrical interconnection of the high permittivity powder particles by the partly crystallized matrix phase.

References

1. CHAE-RYONG CHO, ERWEI SHI, MIN-SU JANG, SE-YOUNG JEONG and SEONG-CHUL KIM, *Jpn. J. Appl. Phys.* **33** (9Apt.l) (1994) 1984.
2. E. SHI, C. R. CHO, M. S. JANG, S. Y. JEONG and H. J. KIM, *J. Mater. Res.* **9**(11)(1994) 2914.
3. T. HOFFMANN, M. GIILTZOW, C. M. SOTOMAYOR TORRES, TH. DOLL and V. M. FUENZALIDA, *Mat. Sci. in Semicond. Proc.* **2** (1999) 335.
4. THOMAS HOFFMANN, THEODOR DOLL and VICTOR M. FUENZALIDA, *J. Electrochem. Soc.* **144**(11) (1997) L292.
5. M. E. PILLEUX and V. M. FUENZALIDA, *J. Appl. Phys.* **74**(7) (1993) 4664.
6. V. M. FUENZALIDA, M. E. PILLEUX and I. EISELE, *Vacuum* **55** (1999) 81.
7. NOBUO ISHIZAWA, HIDEKUNI BANNO, MO-TOO HAYASHI, SEUNG EUL YOO and MASAHIRO YOSHIMURA, *Jpn. J. Appl. Phys.* **29**(11) (1990) 2467.
8. JIANMING ZENG and CHENGLU LIN, *J. Mater. Res.* **14**(7) (1999) 2712.
9. JIANMING ZENG, CHENGLU LIN, JINHUA LI and KUN LI, *Mat. Lett.* **38** (1999) 112.
10. JIANMING ZENG, MIAO ZHANG, ZHITANG SONG, LIANWEI WANG, JINHUA LI, KUN LI and CHENGLU LIN, *Appl. Surf. Sci.* **148** (1999) 137.
11. TAKASHI HYASHI, HIROSHI SHINOZAKI and KYOICHI SASAKI, *J. Eur. Ceram. Soc.* **19** (1999) 1011.
12. R. VIVEKANANDAN and T. R. N. KUTTY, *Powder Tech.* **57** (1989) 181.
13. S. UREK and M. DROFENIK, *Key Eng. Mat.* **132–136** (1997) 125.
14. MIROSLAW M. BUCKO and KRZYSTOF HABERKO, *ibid.* **132–136** (1997) 121.
15. H. NISHIZAWA, N. YAMASAKI, K MATSUODA and H. MITSUSHIO, *J. Am. Ceram. Soc.* **65** (1982) 343.
16. E. TANI, M. YOSHIMURA and S. SOMIYA, *ibid.* **66** (1983) 11.
17. HIROAKI IMAI and HIROSHI HIRASHIMA, *ibid.* **82**(9)(1999) 2301.
18. A. MATSUDA, T. KOGURE, Y. MATSUNO, S. KATAYAMA, T. TSUNO, N. TOGHE and T. MINAMI, *ibid.* **76**(11)(1993) 2899.
19. A. MATSUDA, Y. MATSUNO, S. KATAYAMA, T. TSUNO, N. TOHGE and T. MINAMI, *J. Ceram. Soc. Jpn.* **102** (1994) 330.
20. M. BURGOS and M. LANGLET, *J. Sol-Gel Sci. Tech.* **16**(3) (1999) 267.

Received 8 June
and accepted 12 July 2005